Res Chem Intermed (2018) 44:2405–2423
https://doi.org/10.1007/s11164-017-3237-4

Citronellal cyclisation over heteropoly acid supported on modified montmorillonite catalyst: effects of acidity and pore structure on catalytic activity

Abdul Karim Shah[1,2] · Sungsoo Park[1] · Hassnain Abbas Khan[3] · Umair Hassan Bhatti[4] · Praveen Kumar[1] · Abdul Waheed Bhutto[2] · Yeung Ho Park[1]

Received: 28 December 2016 / Accepted: 14 December 2017 / Published online: 8 January 2018

Abstract Citronellal cyclisation to isopulegol is an important intermediate step in the production of menthol. Several heteropoly acids (PTA) supported on modified montmorillonite (MM) catalysts were synthesized and then tested in cyclisation reactions. The prepared samples were characterized by XRD, ICP-OES, FTIR, N_2 sorption, NH_3-TPD, pyridine adsorption, amine titration and FE-SEM techniques. Effects of post-treatment were studied on montmorillonite pore structure, acidity and catalytic activity. The catalytic activity and isopulegol selectivity improved with acid-treatment and PTA loading. The amount of Lewis acidity of montmorillonite was enhanced with acid-treatment and PTA impregnation. In cyclisation, highest catalytic activity (31.87 mmol cat g^{-1} min^{-1}) was achieved with 96% isopulegol yield in the use of 20% PTA-MM catalyst. The highest catalytic activity and selectivity were obtained in the presence of higher acidity and strong Lewis acidic sites, whereas effects of pore structure blockage seemed minor. The catalytic activity further decreased with the loss of active acidic sites (L and B) due to PTA decomposition with calcination at a higher temperature.

Electronic supplementary material The online version of this article (https://doi.org/10.1007/s11164-017-3237-4) contains supplementary material, which is available to authorized users.

✉ Abdul Karim Shah
drakshah1214@gmail.com; karim@hanyang.ac.kr

[1] Department of Fusion Chemical Engineering, Hanyang University, Sangnok-su, Ansan, South Korea

[2] Department of Chemical Engineering, Dawood University of Engineering and Technology, Karachi, Sindh, Pakistan

[3] Clean Energy and Chemical Engineering, University of Science and Technology, Daejeon, South Korea

[4] Green Energy Process Laboratory, Korea Institute of Energy Research, University of Science and Technology, Daejeon, South Korea

Keywords Acidity · Citronellal cyclisation · Heteropoly acids · Isopulegol · Montmorillonite · Pore structure

Abbreviations

S_{BET}	Specific surface area
V_{total}	Total pore volume
V_{meso}	Mesopore volume
Ds	Stereo-selectivity of (±) isopulegol
MT	Montmorillonite
MM	Acid-treated montmorillonite
PTA	Phosphotungstic acid
PTA-MM	Heteropoly acid supported acid-treated montmorillonite
L.A	Lewis acid sites
B.A	Brønsted acid sites
BET	Brunauer–Emmet–Teller
FTIR	Fourier transforms infrared spectroscopy
ICP-OES	Inductively coupled plasma optical emission spectrometry
XRD	X-ray diffraction

Introduction

Citronellal and isopulegol are important precursors for the synthesis of menthol, which has important applications in pharmaceuticals, cosmetics, fragrances and the tobacco industry [1–3]. The acid catalyzed cyclisation of citronellal to isopulegol (Scheme 1) is an important part of the synthetic route in the production of menthol.

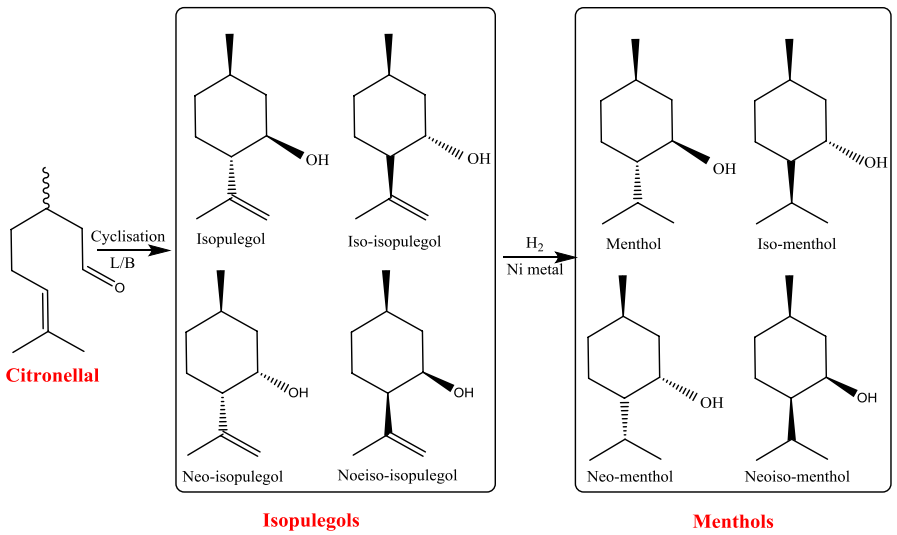

Scheme 1 Cyclisation of (±) citronellal to isopulegol, followed by the hydrogenation to menthols

Different stereoisomers of isopulegol such as (±)-isopulegol, (±)-neo-isopulegol, (±)-iso-isopulegol, and (±)-neoiso-isopulegol (Scheme 1) are formed during cyclisation of citronellal. Further hydrogenation of these isopulegol isomers lead to four pairs of enantiomers: (±)-menthol, (±)-neo-menthol, (±)-iso-menthol, and (±)-neoiso-menthol. Among these isomers, (−)-menthol has a peppermint odor and exerts a cooling effect.

The cyclisation of citronellal has already been studied over various homogeneous and heterogeneous catalysts. In previously published reports, different homogeneous catalysts such as scandium trifluoromethane sulfonate, Lewis acids such as $ZnCl_2$, $ZnBr_2$, and ZnI_2, and molybdenum and tungsten complexes were found to be active in the reaction. Among these catalysts, $ZnBr_2$ showed a high selectivity for (−)-isopulegol, 94%, and has been used at industrial scale [1, 4]. Similarly, scandium trifluoromethane sulfonate was found to be an efficient catalyst for selective cyclisation of citronellal to isopulegol under sub-ambient temperatures. At – 78 °C, a yield of isopulegol of about 95% was obtained. In contrast, the yield at room temperature was only 58% because of the consecutive reaction of the formed isopulegol with citronellal [5]. Recently, Takasago International Corporation obtained 100% selectivity for isopulegol over substituted tris(2,6-diarylphenoxy)aluminum catalyst, but, the bulky ligand group resulted in decreases in isopulegol selectivity and formed other isomers of isopulegol. While homogenous catalysts offer advantages, there are some drawbacks such as difficulty in catalyst recovery, toxicity, weak stability and disposal problems. On the basis of homogeneous catalyst problems, a number of solid acid heterogeneous catalysts (Lewis or Brønsted acidic in nature) have been applied in this reaction for a getting higher selectivity of isopulegol [12]. These include CMS [6], hydrous zirconia [1], zeolites and mesoporous materials [7], solid Lewis acids [8], HPW-SiO_2 [9], inorganic fluorides [10] and HPW-MCM-41 [11], MCM-22, mordenite, alumina, mixed oxides of SiO_2–TiO_2, SiO_2–ZrO_2 and SiO_2–Al_2O_3 and metal cation-exchanged montmorillonite, but some of these seem less active and selective in this reaction [10, 13]. In cyclisation, catalytic activity and isopulegol selectivity appear to be more dependent on Lewis or Brønsted acidity of the catalyst. Cyclisation has also been carried out over SiO_2 at 25 °C with 83% yield in 2 h [14]. A previous study suggested that Lewis acidic catalysts are more efficient in the synthesis of isopulegol, but a huge quantity of catalyst was used. Fuentes et al. [15] used different zeolites in cyclisation and found a correlation of activity with strength and pore size of Brønsted acid sites. Zeolites of small pore size resulted in low activity, whereas, zeolites of larger pore size caused a decrease in selectivity because of more access to Brønsted acid sites, which facilitates more dehydration and cracking of isopulegol. However, Zr-exchanged montmorillonite was found to be more efficient in citronellal cyclisation and gave 91% yield within 24 h with less formation of side products [16]. In addition, pore structure, acidity and nature of acidic sites have a key effect on catalytic activity and selectivity in cyclisation. Still, the nature of the acidic sites have remained unclear, as the activity and selectivity have been correlated either with Lewis or Brønsted acidity. It might be worthwhile to utilize more acidic catalysts such as a heteropoly acid (HPA). HPAs have Keggin structures, strong redox nature and super acidic properties [13, 17–21]. For this investigation, some catalysts of different acidic natures were synthesized using heteropoly acids.

Phosphotungstic acid (PTA) is the most stable among all HPAs and is commonly used for acid catalysis, since it possesses the highest Brønsted acidity [22–24]. In homogenous liquid phase catalysis, the advantages of the HPAs are unique due to their volatility, high acidity, low corrosiveness, and flexibility [25]. Their industrial applications, however, have been limited due to their low surface area (1–10 $m^2\ g^{-1}$) and recovery problems [13, 26–28].

Montmorillonite clays, micro-layered silicates, can be used as a different support for HPA since they are used as inorganic supports for reagents or catalysts in numerous organic reactions [29–33]. Montmorillonite has been modified with different metals and applied to different reactions [18, 34–42]. It might be worthwhile to treat montmorillonite with acid to remove extraneous materials from the inside and improve mass transfer and acidity. Therefore, fine and uniform dispersion of PTA on acid-treated montmorillonite will increase acidity and catalytic activity. From the literature, we found that HPAs supported on acid-treated montmorillonite have been applied to esterification of acetic acid with sec-butanol, esterification of acetic acid with butanol [43] and dehydration of dilute bio-ethanol [44]. This type of catalytic system, however, has not yet been utilized in the citronellal cyclisation reaction. The novelty of this work is to resolve mass transfer limitations and recovery problems of montmorillonite and heteropoly acid, respectively, through acid-treatment and PTA impregnation.

In this research work, we tried to investigate major changes in pore structural and acidic (acidity strength and Lewis/Brønsted acid sites) characteristics of montmorillonite after acid-treatment and heteropoly acid impregnation, and we further investigate their correlation with catalytic activity and selectivity in citronellal cyclisation. In this regard, we prepared heterogeneous acid catalysts through acid-treatment of montmorillonite, HPA impregnation, and calcination temperature. The active and selective catalyst was prepared especially for cyclisation reaction. In comparison with our prepared catalysts, commercially available catalysts such as Al_2O_3, USY, H-MCM-41, and ZSM-5 have been tested analytically and compared.

Experimental

Materials and methods

Phosphotungstic acid hydrate, one of the HPAs (PTA, $H_3PW_{12}O_{40}{\cdot}nH_2O$), montmorillonite (K10), alumina neutral, pyridine anhydrous (99.8%), (±) citronellal (≥ 95% pure) and hydrochloric acid solution (4 M HCl in H_2O) were supplied by Merck. Benzene, nitrobenzene (99.5%) and methanol (99.8%) were purchased from Dae-Jung Chemicals and used as received without further purification. For comparative study, USY (CBV 780, Si/Al = 80) and ZSM-5 (CBV-5524G with Si/Al = 50) were purchased from Zeolyst International USA. MCM-41 (Si/Al = 5) was purchased from Nankai Plant, China.

Catalyst preparation

A series of catalysts having 5, 10, 20 and 30% loadings of PTA on the acid-treated support were synthesized in three steps: (1) the preparation of the support by an acid treatment of montmorillonite, (2) impregnation of PTA on the support and (3) thermal treatment of the catalyst. The original montmorillonite (which will be designated as 'MT') was treated with 4 M HCl (20 mL g^{-1}) and heated to 80 °C for 2 h under reflux conditions. The acid-treated montmorillonite was then washed and neutralized with distilled water, dried overnight and calcined at 200 °C for 2 h (the result of which will be designated as 'MM'). The different loadings (5–30%) of heteropoly acids (PTA) were then impregnated on the acid-treated montmorillonite 'MM' in methanol by wet impregnation [13, 44]. The resulting solids were evaporated and dried at 60 °C for 12 h. (These catalysts were labeled as *x*%-PTA-MM catalyst, where *x* is the PTA loading amount). Some of the prepared catalysts were further calcined at other high temperatures (200–750 °C) in order to determine their catalytic behavior. These catalysts were designated as 'wt%PTA-MM-*y*', whereas; *y* shows calcination temperature.

Catalyst characterization

XRD patterns of all samples were collected through Powdered X-ray diffraction (D/Max 2200 Rigaku) using Cu Kα radiation at a fixed accelerating voltage (40 kV) and current (100 mA) within the 2θ range of 5°–60°. ICP-OES was used to determine the elemental composition of samples with HPA deposition amount using an Optima 8000. For elemental analysis, a 0.1 g quantity of each sample was dissolved in 1 mL of 36% HCl, 1 mL of 70% HNO_3, 0.5 mL of 60% HF and 4 mL of H_2O. After being complete dissolved, HF was neutralized with 2 g of boric acid. Afterwards, this digested mixture was further diluted with water to get the desired concentration (1 ppm) [45]. The surface area, pore volume, and pore size distribution were measured by nitrogen adsorption using a Micrometrics Tri-Star 3020. Before the measurement, all samples were degassed at 200 °C for 3 h under vacuum conditions, and micropore volume of all samples was determined by the t-plot method. For finding changes in surface morphology of samples, SEM images were collected through a field emission scanning electron microscope FE-SEM, MIRA-3 Tescan, South Korea. Before this analysis, all samples were prepared on graphite carrier and then coated with a 3 mm layer of platinum. During SEM analysis, the SEM–EDX characterization was done through FE-SEM, MIRA-3, equipped with EDX-micro analyzer EX-350. The acidity of samples was measured by NH_3-Temperature-Programmed Desorption (TPD) using an Auto-Chem 2920, Micrometrics, USA. Adsorption of NH_3 was performed at 50 °C temperature with a flow rate of 20 cm^3 min^{-1} for 45 min, followed by helium purging for 1.5 h at room temperature in order to remove the physisorbed NH_3. The desorption process was recorded in the temperature range of 50–900 °C at a heating rate of 10 °C min^{-1} under a helium flow (20 cm^3 min^{-1}), and the evolved NH_3 was monitored by TCD. In comparison with NH_3-TPD data, the acidity amount of samples was determined through the amine titration technique

as described in procedure [46] using 0.1 N butyl amine (in dry benzene) solution as a weak base and dimethyl yellow as an indicator. Each catalyst sample (0.1 g) was dissolved in 9 mL dry benzene and 2–3 drops of indicator were added in the catalyst solution. The dissolved catalyst solution was titrated with 0.1 N *n*-butyl amine solution until the color changed from pink to yellow. The solution was continuously stirred for 4 h and titrated again with butyl amine to achive complete saturation. Total volume (mL) of the consumed titrant was recorded, and the acidity amount was calculated. For the measurement of acidic sites of samples, a KBr mixed FTIR pellet (55 mg) was prepared using a hydraulic pressing machine (11 tons pressure, 3 min). The pellet was fixed inside a stainless steel IR cell and dehydrated at 300 °C for 2 h under a vacuum system using 5 °C min^{-1} temperature ramp. The IR cell was then connected with the FTIR equipment in order to collect a visible spectrum of the sample using 600–4000 cm^{-1}, 8 cm^{-1} optical resolution and co-addition of 32 scans through FTIR equipment. Next, pyridine vapors were introduced into the IR cell until pyridine pressure became 10 kPa. Pyridine adsorption was performed at 100 °C for 2 h. After complete pyridine adsorption, physisorbed pyridine was removed at 150 °C under vacuum conditions. FTIR apparatus was connected for measurement of the IR spectrum under similar conditions [47]. The quantitative amount of acidic sites was calculated using the following formula:

$$\begin{aligned} C(\mathrm{L}) &= 1.42 * \mathrm{IA(LA)} * R^2/W_{\mathrm{cat}} \\ C(\mathrm{B}) &= 1.88 * \mathrm{IA(BA)} * R^2/W_{\mathrm{cat}} \end{aligned},$$

where C(L) and C(B) show concentration of Lewis and Brønsted acid sites, respectively, and IA (L) and IA (B) indicate integrated surface areas of Lewis and Brønsted acid sites peaks (1440 and 1540 cm^{-1}), respectively. R is the radius of the pellet and W_{cat} is the total amount of catalyst which was used in the preparation of the KBr pellet.

Catalytic cyclisation of citronellal

The cyclisation of the citronellal reaction was carried out in a glass reactor consisting of a 10 mL glass vial, a rubber septum, a magnet and a plastic cap. A specific amount of chemicals, such as 4.5 mmol of (±) citronellal (≥ 95%), 0.2 mL nitrobenzene (internal standard), 5 mL benzene solvent and 5.5 mg catalyst, were poured into glass vial and the cap tightened. Before the start of the reaction, a silicon oil bath system was heated and its temperature was maintained up to 40 °C. All glass reactors were fixed inside the heating bath. The reaction proceeded for 1 h and reaction sampling was done at different times (3–60 min) in order to analyze the catalytic conversion of citronellal. GC analysis of reaction samples was done by chiral column (Cyclodex-B, length 60 m, diameter 0.254 mm and film thickness 0.25 μm). Helium was used as the carrier gas. The products were separated by the following temperature program: 95 °C (1 min), 0.3 °C min^{-1}, 120 °C (1 min), 15 °C min^{-1} and 220 °C (1 min) with a split ratio of 100:1. The detector and injector temperatures

were 280 and 250 °C, respectively. The reaction products and isomers were further identified by GC–MS with a triple axis detector (Agilent, Model No. 7890A) and GC chemical standards.

Results and discussion

Textural and acidic properties

During acid-treatment of montmorillonite (MT), some amount of Al was removed from the montmorillonite framework in accordance with ICP-OES data, and then more siliceous support (MM) was prepared (Table 1), which resulted in more enhancements in mesopore surface area. This enhancement in support might be related to the removal of some of the aluminum from octahedral sites of montmorillonite [48, 49]. The specific amount of PTA was doped on 'MM' support as well, but less than actual loading (Table 1). The XRD crystalline structure of 'MT' was maintained even after acid-treatment and PTA impregnation, and minor changes in XRD pattern were seen (Fig. 1). Some XRD peaks of heteropoly acid ($2\theta = 10°$, 25°, 37° and 60°) were seen on the 'MM' surface after PTA deposition, but intensities of PTA were rather low, which might be due to high dispersion of PTA over the support (Fig. 1).

FTIR analysis

In the FTIR spectra, bulk PTA shows the characteristic IR bands at 1071 cm^{-1} (P–O in central tetrahedral), 975 cm^{-1} (terminal W = O), 813 cm^{-1} and 900 cm^{-1} (W–O–W) associated with the asymmetric vibrations of the Keggin polyanions (Fig. 2). After PTA was deposited on the MM support, some of the characteristic Keggin bands were observed at 812, 900 and 986 cm^{-1} , as well as other bands, merged with those of montmorillonite, producing a single broad IR peak (Fig. 2). The changes in IR spectrum of 'MM' indicate successful deposition of PTA on the 'MM' surface.

BET analysis

The mesopore surface area (164–188 $m^2\ g^{-1}$), mesopore volume (0.24–0.29 $cm^3\ g^{-1}$) and mesopore size (3.8–5.5 nm) of 'MT' increased after acid-treatment (Table 1). Significant changes in the pore structure of the 'MT' were seen, which might be due to Al removal from the main framework of montmorillonite (Fig. 3). However, the increase in PTA loading on the support (MM) caused a decrease in the specific mesopore surface area (188–88 $m^2\ g^{-1}$) and mesopore volume (0.29–0.17 $cm^3\ g^{-1}$), respectively. High mesopore surface area of the support (MM) might be related to the removal of some of the aluminum from octahedral sites of montmorillonite. The mesopore surface area and mesopore volume decreased with PTA loading, which may be due to the blockage of pores by PTA molecules. The pore size of 'MT'

Table 1 Textural and acidic properties of solid acid catalysts

Catalyst	S_{meso}[a] ($m^2\ g^{-1}$)	V_{meso}[a] ($cm^3\ g^{-1}$)	Dp (Nm)	Acidity (μmol g^{-1} cat)			Acidic sites[d]			ICP-OES[e] (%)
				Amine titration[b]	NH_3-TPD[c]	Lewis acid sites	Brønsted acid sites	B + L	B/L	
MT	164	0.24	3.8	0.51	0.31	89	14	104	0.16	830[f]
MM	188	0.29	5.5	0.54	0.44	123	7	130	0.06	746[f]
10% PTA-MM	174	0.28	5.8	0.80	1.02	150	51	201	0.34	7.1[g]
20% PTA-MM	145	0.22	6.6	1.32	1.35	229	106	335	0.46	15.g[g]
30% PTA-MM	88	0.17	7.6	1.54	1.40	219	138	357	0.63	26.7[g]

[a]Determined by BJH method

[b]Determined by amine titration

[c]Determined by NH_3-TPD technique

[d]Determined by pyridine adsorption IR spectroscopy

[e]Determined by ICP-OES technique

[f]Al content (μL^{-1})

[g]PTA loading (%)

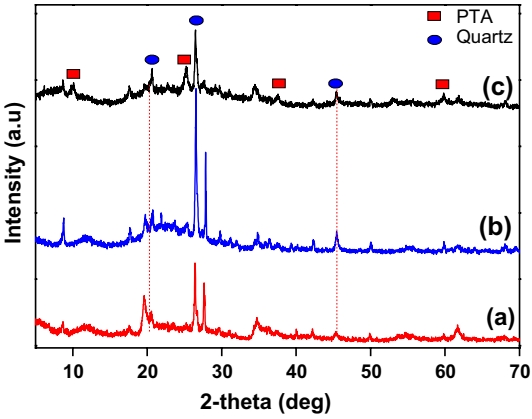

Fig. 1 XRD patterns of *a* MT, *b* MM and *c* PTA-MM samples

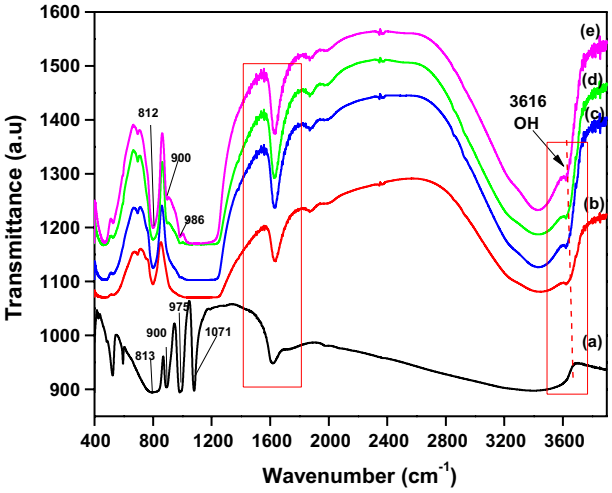

Fig. 2 FTIR spectra of *a* pure PTA, *b* MM, *c* 10% PTA-MM, *d* 20% PTA-MM and *e* 30% PTA-MM. This graph shows deposition of Keggin structure components (IR bands at 800, 894, 980 and 1080 cm^{-1}) on the acid-treated montmorillonite surface

improved with acid treatment and PTA loading (Table 1). The pore size distribution (BJH) of all samples show that average pore sizes of 'MT' and other samples are in the range of 3.8–7.6 nm, suggesting that catalysts lie in the mesoporous region in the presence of micropores (Table 1). The adsorption–desorption isotherms of MM and supported PTA catalysts, shown in Fig. 3, have a hysteresis loop of isotherms type I and IV, which shows the characteristic of the micro-mesoporous material. In addition, these results are in agreement with adsorption data which shows that the pore volume, as well as mesopore volume, of the 'MT' was enhanced with acid-treatment, but lessened with PTA loading.

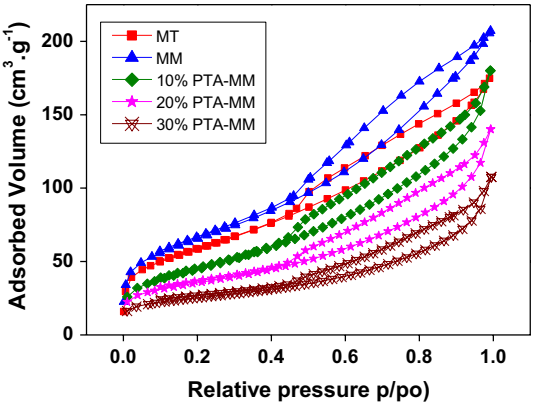

Fig. 3 N_2-adsorption desorption isotherms of prepared samples

SEM analysis

In Fig. 4, FE-SEM images indicate that montmorillonite is a layered clay consisting of octahedral aluminate modules and tetrahedral silicate modules [1]. After successful impregnation of PTA, the surface morphology of MM changed and layers were deteriorated; no more thin and long layers were seen. Furthermore, FE-SEM–EDX shows the elemental composition of MT, which contains Si, Al and Mg, whereas the intensity of Si and Al decreased after acid treatment as shown in Online Resource 2.

The acidity strength of samples was determined by NH_3-TPD and amine titration techniques, respectively, as shown in Table 1. The original montmorillonite 'MT' contains a specific amount of acidity. Further acidity strength of 'MT' was enhanced (0.31–1.40 μmol g^{-1} cat) with acid treatment and PTA loading. However, similar observations were seen in acidity enhancement as compared to amine titration

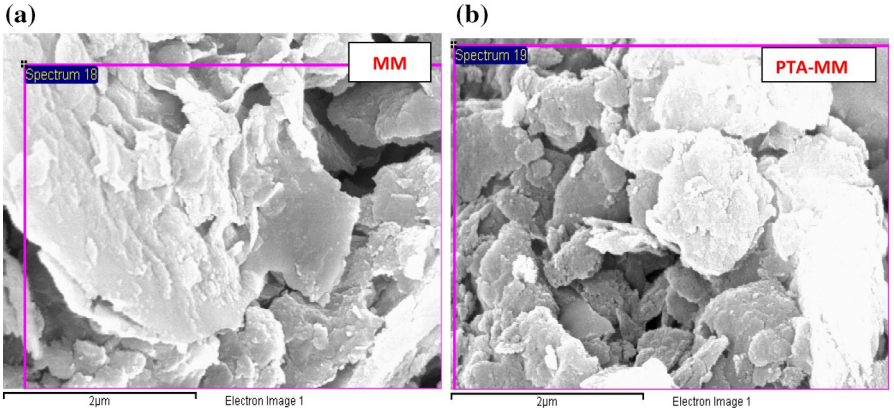

Fig. 4 SEM images of **a** MM, **b** 20%PTA-MM samples

analysis data (Table 1). The analysis revealed that acid-treatment and PTA impregnation treatments were found to be more effective in enhancing acidity strength of 'MT'.

Pyridine analysis

Pyridine adsorption spectroscopy was used to determine the nature and strength of acidic sites [50], as shown in Table 1 and Fig. 5. Bands in the range of 1440–1454, 1480–1500 and 1540–1640 cm^{-1} indicate the presence of both hydrogen-bonded and co-coordinately bonded pyridine, respectively. 'MT' contains medium Lewis and weak Brønsted acidic sites. After acid treatment of MT, the number of Lewis acid sites increased with a decrease in the number of Brønsted acid sites. However, the number of Lewis acid sites further increased with increases in PTA amount. After PTA loading, an increase in acidity was seen, designated by a slight shift of the bands to high wavenumbers and an increase in the absorbance of the 1485 and 1540 cm^{-1} band. In addition, a weak band centered at 1540 $cm^{-1}$is suggestive of Brønsted acidic sites for PTA supported samples. However, with a further increase in PTA loading above 20%, the number of Brønsted acid sites increased with a decrease in Lewis acid sites (Table 1; Fig. 5).

Similarly, the number of Lewis and Brønsted acid sites sharply decreased with the use of higher calcination temperature (Table 3). Similarly, the peaks of water adsorbed (1640 cm^{-1}) and hydroxyl groups (3640 cm^{-1}) increased with PTA loading (Fig. 2), and further decreased with increase in calcination temperature (Online Resource 7). This might be due to dehydration or dehydroxylation of the catalyst. Furthermore, total acidity amount (1.32–0.153 mmol g^{-1} cat) of 20% PTA-MM decreased with an increase in calcination temperature due to loss of PTA molecules (Table 3 and Online Resource 6). The mesopore surface area (145–49 m^2 g^{-1}) of 20% PTA-MM catalysts rigorously decreased with increases in pore size (Table 3). These data are in agreement with XRD and FTIR spectra, which show some signs

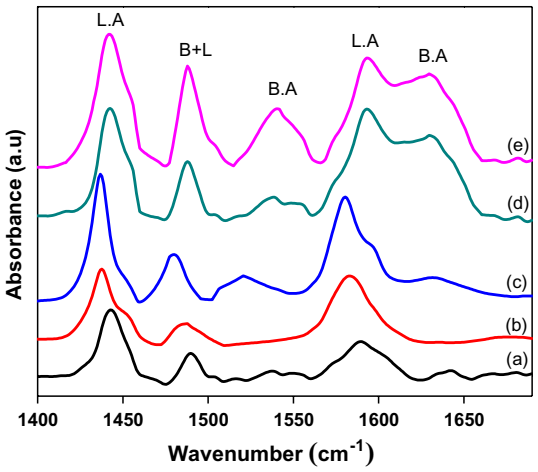

Fig. 5 Pyridine adsorbed IR spectra of *a* MT, *b* MM, *c* 10% PTA-MM, *d* 20% PTA-MM and *e* 30% PTA-MM catalysts

of PTA decomposition. More data about calcination temperature effects on textural, acidic and catalytic properties are provided in Online Resources 5–8. The detailed experimental observation reveals that high calcination temperature is not suitable for a getting highly active and selective catalyst for the cyclisation reaction.

Catalytic activity

Table 2 shows the conversion of (±) citronellal and the selectivity towards isopulegol over the prepared samples. The catalyst amount was found to be within 0.8% for the reaction. The different isomers were recognized by GC grade chemicals and GC-MSD. All the heteropoly acid supported catalysts gave (±)-isopulegol as the predominant isomer, followed by (±)-neo-isopulegol, (±)-iso-isopulegol, and (±)-neoiso-isopulegol (Table 2).

The catalytic citronellal cyclisation reaction was conducted in glass type reactors, and reaction performance of several catalysts was evaluated. In the first instance, phosphotungstic acid hydrate (PTA) was tested, which gave 41% conversion with 53% selectivity within 1 h. It was highly soluble in benzene solvent and its recovery seemed difficult. The montmorillonite (MT) sample exhibited catalytic characteristics that resulted in 54% citronellal conversion with 70% isopulegol production within 1 h. Further, the catalytic activity (72.4%) and selectivity (81%) were enhanced drastically when the MT sample was treated with HCl (Table 2). The poor catalytic performance of the MT sample might be related to the narrow pore structure and weak acid sites (Lewis or Brønsted) (Table 1). It has been observed that pore structure and Lewis acid site strength of the MT sample was improved after

Table 2 Results of citronellal cyclization on various PTA supported catalysts

Catalyst type	Catalytic activity[a] (mmol g^{-1}, min^{-1})	Conversion[b] (%)	Yield[c] (%)	Selectivity (%)	Isomers distribution (%)[d]			Ds (%)
					2a	2b	2c	2a
PTA	6.8	41	21.7	53	35	13	5	66
MT	7.6	54.12	37.8	70	52	14	4	74
MM	9.99	72.4	58.6	81	64	12	5	79
5% PTA-MM	13.13	91.1	84.7	93	75	15	3	81
10% PTA-MM	17.38	95.3	89.6	94	75	16	3	80
20% PTA-MM	31.87	100	95.5	96	78	15	2	82
30% PTA-MM	29.6	100	94	94	77	16	1	82

[a]Determined by total moles of citronellal * total conversion * molecular weight of citronellal divided by 100 * catalyst amount * reaction time

[b]Reaction conditions: 4.275 mmol (±) citronellal, 5 mL C_6H_6, 0.2 mL $C_6H_5NO_2$, 5.5 mg catalyst, 40 °C, 1 h

[c]Yield of isopulegol was calculated by total conversion multiplied by overall isopulegol selectivity (2a–2d) divided by 100

[d](±) isopulegol (2a): (±) neo-isopulegol (2b), (±) iso-isopulegol (2c)

acid treatment, resulting in enhancement in catalytic activity and selectivity. When PTA was impregnated on the MM support, higher catalytic activity and selectivity were achieved than in MM and MT samples. The 5–30% PTA-MM catalysts were very active with 91–100% conversion of citronellal, and their initial catalytic activity was about 13.13–31.87 mmol cat g^{-1} min^{-1}. Furthermore, the selectivity over these catalysts was very high, 93–96%, with only a small fraction of the isopulegol undergoing successive dimerization to ethers. The initial reaction rate of these catalysts was very high up to 3 min, then their catalytic activity rate decreased with reaction time (Fig. 6).

However, when a PTA amount was impregnated on MM, the amount of Lewis acidity increased, leading to high catalytic activity and selectivity. Among these samples, 20% PTA-MM catalyst was found to be a more active and selective catalyst for citronellal cyclisation (100% conversion and 96% selectivity) (Table 2).

The 20% PTA supported MM catalyst retained high selectivity and catalytic activity, which could be due to the micro-mesoporous nature of catalyst and the presence of strong Lewis acidity combined with weak Brønsted acidity [1]. The incorporation of PTA on the MM surface changes its acidic property. Indeed, when MT was modified through acid-treatment and PTA deposition, the resulting material, 20% PTA-MM, was catalytically active for the cyclisation reaction (Table 2), even though it possessed low mesopore surface area. This catalyst prepared by PTA impregnation under normal drying (60 °C) was highly active in the synthesis of isopulegol. The increase in Lewis acidity was a key factor for enhancing catalytic activity and selectivity. When 30% PTA was impregnated on the MM support, the catalytic activity (29.6 mmol cat g^{-1} min^{-1}) and selectivity (94%) decreased slightly compared to the 20% PTA-MM sample, because ofa decrease in mesopore surface area and an increase in Brønsted acidity. About 6% of by-products were formed, which might be due to dehydration and cracking of isopulegol.

After finding optimum loading of PTA, 20% PTA-MM catalyst was found to be more active and selective for cyclisation, so this catalyst was calcined at different calcination temperatures (200–750 °C) in order to determine the catalytic activity behavior with respect to their acidic properties (Table 3). The catalyst which was

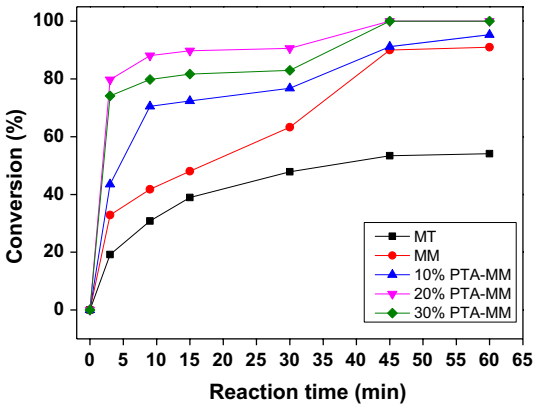

Fig. 6 Reaction performance of solid acid catalysts in citronellal cyclisation reaction. This reaction was performed at 40 °C using 0.7 g citronellal, 5 mL Benzene and 5.5 mg catalyst

Table 3 Catalytic activity and characterization data of calcined PTA-MM catalysts

Calcined (°C)	Activity rate[a] (min^{-1})	Conversion[b] (%)	Selectivity (%)	Acidity[c] (mmol g^{-1} cat)	Acidic sites[d]				S_{meso}[e] (m^2 g^{-1})
					Lewis	Brønsted	B + L	B/L	
60	31.87	100	95	1.32	229	106	335	0.46	145
200	29.2	92	95	0.89	121	71	181	0.65	142
400	5.99	54.8	92	0.36	114	24	138	0.21	136
600	5.65	22.3	90	0.23	103	19	122	0.18	114
750	4.98	17.1	86	0.15	53	15	68	0.29	49

[a]Determined by total moles of citronellal * total conversion * molecular weight of citronellal divided by 100 * catalyst amount * reaction time

[b]Reaction conditions: 4.275 mmol (±) citronellal, 5 mL C_6H_6, 0.2 mL C6H5NO2, 5.5 mg catalyst, T 40 °C, 1 h

[c]Determined by amine titration technique

[d]Determined by pyridine adsorption IR spectroscopy

[e]Determined by BJH method

calcined at 200 °C showed a good catalytic activity (29.2 mmol cat g^{-1} min^{-1}) and selectivity (95%), but less than that of 20% PTA-MM that was dried at 60 °C. This decreasing effect was due to a slight decrease in mesopore surface area, acidity, Lewis and Brønsted acid sites, because of dehydration. This decreasing trend seemed proportional with an increase of calcination temperature up to 750 °C. However, the catalytic activity and selectivity further decreased with increases in calcination temperature because of dehydroxylation and PTA decomposition [51]. More loss of mesopore surface area, acidity or acidic sites results in greater decreases in catalytic activity and selectivity.

Experimental data suggest that high acidity strength, strong Lewis and weak Brønsted acid sites can be considered to be the main tools for a achieving higher catalytic activity and selectivity. However, acidity strength of MT and Lewis acid site intensity increased after acid treatment and PTA impregnation. The catalytic activity and selectivity of MT was enhanced (7.6–31.87 mmol g^{-1} min^{-1}) with more amelioration in acidity strength (0.31–1.35 μmol g^{-1} cat). The acidity strength and quantitative number of acid sites (L or B) have a direct relation to each other in this reaction. Strong Lewis acid sites are considered to be effective for getting high isopulegol selectivity in cyclisation [1]. Experimental data reveal that enhancement in surface area and pore volume results in a positive contribution to catalytic activity, whereas the severe blockage of pore structure of the catalyst has a negative impact on catalytic performance in the cyclisation reaction. The linear connectivity relationship of catalytic activity with acidity strength, Lewis/Brønsted acid sites ratio and mesopore volume are shown in Fig. 7.

In order to check the reusability of the optimum catalyst (20% PTA-MM) after reaction, it was filtered with a membrane filter, further washed with 50 mL benzene solvent and introduced into the reactor with fresh reaction mixture. Citronellal conversion was 100% in the first run, then decreased to 95% in the second run, further

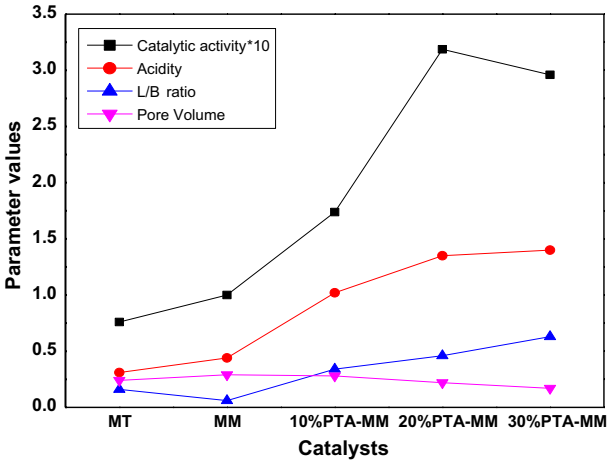

Fig. 7 Linear connectivity relationship of catalytic activity with acidity strength, L/B ratio and pore volume characteristics

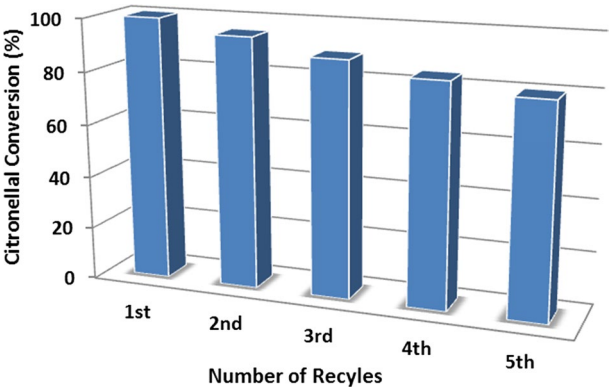

Fig. 8 Recyclability test of 20% PTA-MM catalyst in citronellal cyclisation

Table 4 Comparative study of PTA-MM catalyst with other solid acid catalysts

Catalyst	Conversion[a] (%)	Selectivity (%)	Acidity (mmol g^{-1})		S_{meso}[d] (m^2 g^{-1})
			Amine titration[b]	NH_3-TPD[c]	
Al_2O_3	7.0	46	0	0	107
MCM-41 (Si/Al = 5)	68	95	0.16	0.65	1137
USY (Si/Al = 80)	78	88	0.44	1.14	135
ZSM-5 (Si/Al = 50)	25	90	0.65	1.25	47
20% PTA-MM	100	96	1.32	1.35	145

[a]Reaction conditions: 4.275 mmol (±)citronellal, 5 mL C6H6, 0.2 mL C6H5NO2, 5.5 mg catalyst, T 40 °C, 30 min

[b]Determined by amine titration technique

[c]Determined by NH3-TPD technique

[d]Determined by BJH method

decreased to 89% in the third run and finally decreased up to 80% in the fifth run (Fig. 8). It seems that the activity of the catalyst decreased only slightly with the number of cycles, whereas the loss of catalyst during filtration was under observation. Little variation was seen in isopulegol production during the recyclability test.

Our investigation was extended in order to determine the individual roles of Lewis and Brønsted acid sites in cyclisation. An Al_2O_3 sample was used in citronellal cyclisation in order to evaluate its catalytic performance. However, it showed negligible catalytic activity in citronellal cyclisation (7% conversion and 46% selectivity within 1 h). This poor performance might be related mainly to its weak acidity (Table 4). Furthermore, the pyridine IR studies show that only weak Lewis acid sites were present on the alumina surface. However, individual Lewis acid sites seemed ineffective for a complete cyclisation and higher isopulegol yield formation. For comparison, a mesoporous siliceous material such as MCM-41 was used

in cyclisation in order to determine the effect of mesoporosity on cyclisation. It gave 68% conversion and 95% isopulegol selectivity within 1 h; so this good performance might be related to the presence of medium Lewis acid sites (acidity) with weaker Brønsted sites, as can be seen clearly in Table 4 and Fig. 9. From reaction data, it is clear that higher mesopore surface area (1137 $m^2\ g^{-1}$) had no direct effect on catalytic activity as compared with other samples. We investigated further to determine the effects of strong Brønsted acidic sites through pyridine adsorption on catalytic activity and isopulegol selectivity. Ultra stable zeolite Y (USY) and ZSM-5 zeolites of different pore structured materials were used in this reaction. The USY showed good catalytic activity (conv. 78%) and selectivity (88%) when compared with the ZSM-5 catalyst (conv. 25% and selectivity 90%), because USY contains medium intensity of Lewis sites with a higher mesopore surface area (135 $m^2\ g^{-1}$) as compared to ZSM-5 (47 $m^2\ g^{-1}$). In the use of USY catalyst, about 12% of the total isopulegol amount was cracked or dehydrated into other by-products, due to the presence of strong Brønsted acid sites. ZSM-5 showed poorer catalytic activity than USY, even though it contained a higher amount of acidity. So, this poor performance of ZSM-5 might be due to the presence of weak Lewis and strong Brønsted acid sites and a small mesopore surface area. Experimental data and previous work [1] suggest that citronellal cyclisation to isopulegol occurs through protonation–deprotonation mechanism with the help of strong Lewis and weak Brønsted acid sites. When citronellal molecule binds with Lewis acid site via the aldehyde oxygen. This brings the citronellal into an orientation favourable for ring closure through an intramolecular carbonyl-ene (C–C) reaction. In the transition state, protonation of the oxygen occurs via a neighbouring Brønsted hydroxyl group, together with an abstraction of hydrogen from the isopropyl group followed by ring closure to form isopulegol.

In comparison, PTA-MM catalyst was found to be more active and selective than other catalysts, because of high acidity strength, strong Lewis and weak Brønsted acid sites. This study suggests that mesopore surface area and pore size might have negligible effects in the cyclisation reaction, whereas high acidity strength and strong Lewis acid sites in the presence of weak Brønsted acid sites have major

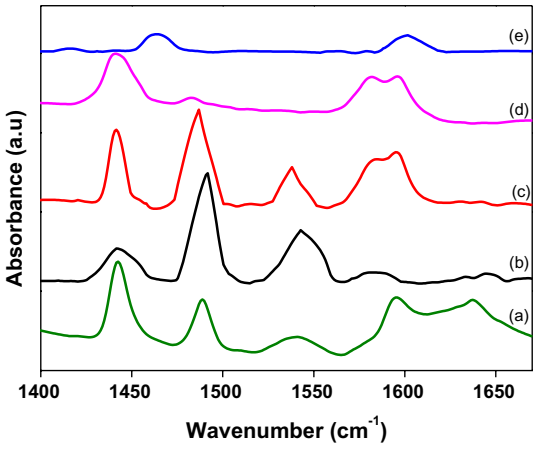

Fig. 9 Pyridine adsorbed IR spectra of *a* PTA-MM, *b* ZSM-5, *c* USY, *d* MCM-41 and *e* Al_2O_3

effects on catalytic activity and selectivity. However, the catalytic activity increased with an increase in the number of Lewis acid sites, but decreased with an increase in the number of Brønsted acidic sites with loss of Lewis acid sites. Furthermore, strong Lewis and weak Brønsted acid sites are necessary to promote efficient citronellal cyclisation. In addition, the mere presence of Lewis acid sites on catalyst surface seemed insufficient for achieving complete conversion of citronellal to isopulegol in cyclisation. Continuing this reaction for a long time, some by-products were formed. This side product formation was possible through dehydration, etherification or cracking of isopulegol over strong acidic sites of the catalyst.

Conclusion

In this research, efficient solid acid catalysts were prepared through acid-treatment of montmorillonite (MT) and impregnation of a heteropoly acid, $H_3PW_{12}O_{40}$ (PTA) and then were applied in citronellal cyclisation for isopulegol synthesis. The catalysts were characterized by XRD, ICP-OES, FTIR, N_2 sorption, NH_3-TPD, pyridine adsorption, amine titration and FE-SEM techniques. After acid-treatment of montmorillonite, the catalytic activity and selectivity improved due to increases in Lewis acidity and mesopore surface area. The amount of acidity, Lewis, and Brønsted acidic sites was enhanced with an increase in PTA loading. The catalytic activity and isopulegol selectivity significantly improved with an increase in acidity and Lewis acidic sites (with PTA loading), whereas the effect of pore structure blockage in citronellal conversion seemed minor. In the cyclisation reaction, 20% PTA loading on modified montmorillonite was found to be the optimum for achieving higher catalytic activity in citronellal cyclisation (100% conversion, 96% yield, and initial catalytic activity 31.87 mmol cat mg^{-1} min^{-1}). In addition, the highest isopulegol selectivity (96%) was achieved in to the presence of strong Lewis and weak Brønsted acid sites on the catalyst surface. The catalytic activity decreased with 30% PTA loading on montmorillonite due to an increase in the number of Brønsted acidic sites and blockage of pore structure. The total acidity and mesopore surface area decreased with increases in calcination temperature (200–750 °C), which seemed to be due to PTA decomposition. Thermal treatment at 60 °C was found to be the best condition for the preparation of an active and selective catalyst after post-treatment of MT.

Acknowledgements This research was conducted through a mutual collaboration of Higher Education Commission Pakistan and Hanyang University, South Korea.

References

1. G.K. Chuah, S.H. Liu, S. Jaenicke, L.J. Harrison, J. Catal. **200**, 2 (2001)
2. H. Oertling, A. Reckziegel, H. Surburg, H.-J. Bertram, Chem. Rev. **107**, 5 (2007)
3. T. Patel, Y. Ishiuji, G. Yosipovitch, J. Am. Acad. Dermatol. **57**, 5 (2007)
4. P. Kočovský, G. Ahmed, J. Šrogl, A.V. Malkov, J. Steele, J. Org. Chem. **64**, 8 (1999)
5. V.K. Aggarwal, G.P. Vennall, P.N. Davey, C. Newman, Tetrahedron Lett. **39**, 1997 (1998)

6. G.D. Yadav, J.J. Nair, Chem. Commun. **21**, 2369 (1998)
7. P. Mäki-Arvela, N. Kumar, V. Nieminen, R. Sjöholm, T. Salmi, D.Y. Murzin, J. Catal. **225**, 1 (2004)
8. M. Vandichel, F. Vermoortele, S. Cottenie, D.E. De Vos, M. Waroquier, V. Van Speybroeck, J. Catal. **305**, 118 (2013)
9. K.A. da Silva, P.A. Robles-Dutenhefner, E.M.B. Sousa, E.F. Kozhevnikova, I.V. Kozhevnikov, E.V. Gusevskaya, Catal. Commun. **5**, 8 (2004)
10. S.M. Coman, P. Patil, S. Wuttke, E. Kemnitz, Chem. Commun. **4**, 460 (2009)
11. P.R.S. Braga, A.A. Costa, E.F. de Freitas, R.O. Rocha, J.L. de Macedo, A.S. Araujo, J.A. Dias, S.C.L. Dias, J. Mol. Catal. A Chem. **358**, 99–105 (2012)
12. Z. Yongzhong, N. Yuntong, S. Jaenicke, G.-K. Chuah, J. Catal. **229**, 2 (2005)
13. S.K. Bhorodwaj, D.K. Dutta, Appl. Catal. A **378**, 2 (2010)
14. P.J. Kropp, G.W. Breton, S.L. Craig, S.D. Crawford, W.F. Durland, J.E. Jones, J.S. Raleigh, J. Org. Chem. **60**, 13 (1995)
15. M. Fuentes, J. Magraner, C. De Las Pozas, R. Roque-Malherbe, J.P. Pariente, A. Corma, Appl. Catal. **47**, 2 (1989)
16. J.-I. Tateiwa, A. Kimura, M. Takasuka, S. Uemura, J. Chem. Soc. Perkin Trans. **1**, 15 (1997)
17. G.D. Yadav, Catal. Surv. Asia **9**, 2 (2005)
18. S.V. Awate, S.B. Waghmode, K.R. Patil, M.S. Agashe, P.N. Joshi, Korean J. Chem. Eng. **18**, 2 (2001)
19. M. Misono, Korean J. Chem. Eng. **14**, 6 (1997)
20. M. He, A. Pan, J. Xie, H. Li, X. Yuan, X. Cheng, M. Chen, Korean J. Chem. Eng. **29**, 10 (2012)
21. E. Vyskočilová, M. Krátká, M. Veselý, E. Vrbková, L. Červený, Res. Chem. Intermed. **42**, 9 (2016)
22. D.R. Park, U.G. Hong, S.H. Song, J.G. Seo, S.-H. Baeck, J.S. Chung, I.K. Song, Korean J. Chem. Eng. **27**, 2 (2010)
23. E. Rafiee, M. Khodayari, Res. Chem. Intermed. **42**, 4 (2016)
24. Y. Izumi, Res. Chem. Intermed. **24**, 4 (1998)
25. G. Bai, H. Zhang, T. Li, H. Dong, J. Han, Res. Chem. Intermed. **41**, 8 (2015)
26. M.N. Timofeeva, Appl. Catal. A **256**, 1–2 (2003)
27. A. Samzadeh-Kermani, Chem. Mon. **147**, 761–765 (2016)
28. E. Rafiee, N. Nobakht, L. Behbood, Res. Chem. Intermed. **42**, 5573–5585 (2016)
29. J. Safari, M. Sadeghi, Res. Chem. Intermed. **42**, 12 (2016)
30. G.F. Chen, N. Xiao, J.S. Yang, H.Y. Li, B.H. Chen, L.F. Han, Res. Chem. Intermed. **41**, 8 (2015)
31. F.H.J. Al-Shemmari, A.A. Rabah, E.A.J. Al-Mulla, N.O.M.A. Alrahman, Res. Chem. Intermed. **39**, 9 (2013)
32. K. Ravi, B. Krishnakumar, M. Swaminathan, Res. Chem. Intermed. **41**, 8 (2015)
33. M. Kurian, R. Babu, J. Environ. Chem. Eng. **1**, 1–2 (2013)
34. P. Ravindranathan, P.B. Malla, S. Komarneni, R. Roy, Catal. Lett. **6**, 3 (1990)
35. B. Vijayakumar, G. Ranga Rao, J. Porous Mater. **19**, 2 (2012)
36. S. Rostamizadeh, A.M. Amani, R. Aryan, H.R. Ghaieni, L. Norouzi, Chem. Mon. **140**, 5 (2009)
37. Y.-S. Shin, S.-G. Oh, B.-H. Ha, Korean J. Chem. Eng. **20**, 1 (2003)
38. D.-H. Shin, J.-J. Kim, B.-S. Yu, M.-H. Lee, D.-W. Park, Korean J. Chem. Eng. **20**, 1 (2003)
39. A. Samzadeh-Kermani, S. Miri, Korean J. Chem. Eng. **32**, 6 (2015)
40. C.-Y. Ryu, S.-D. Yeo, Korean J. Chem. Eng. **27**, 2 (2010)
41. E. Rafiee, M. Kahrizi, M. Joshaghani, P. Ghaderi-Sheikhi Abadi, Res. Chem. Intermed. **42**, 6 (2016)
42. P. Kar, B.G. Mishra, J. Environ. Chem. Eng. **4**, 2 (2016)
43. S.K. Bhorodwaj, D.K. Dutta, Appl. Clay Sci. **53**, 2 (2011)
44. V.V. Bokade, G.D. Yadav, Appl. Clay Sci. **53**, 2 (2011)
45. V.N. Shetti, J. Kim, R. Srivastava, M. Choi, R. Ryoo, J. Catal. **254**, 2 (2008)
46. M.W. Anderson, J. Klinowski, Zeolites **6**, 3 (1986)
47. E.P. Parry, J. Catal. **2**, 5 (1963)
48. K. Siddhartha, D. Bhorodwaj, D.D. Kumar, Appl. Catal. A **378**, 2 (2010)
49. L. Bieseki, F. Bertell, H. Treichel, F.G. Penha, S.B.C. Pergher, Mater. Res. **16**, 1122–1127 (2013)
50. X. Han, W. Yan, C.-T. Hung, Y. He, P.-H. Wu, L.-L. Liu, S.-J. Huang, S.-B. Liu, Korean J. Chem. Eng. **33**, 2063–2072 (2016)
51. I.V. Kozhevnikov, J. Mol. Catal. A Chem. **305**, 1–2 (2009)